

On avalanche (front) velocity measurements at the Ryggfonn avalanche test site and comparison with observations from other locations

Peter Gauer*

Norwegian Geotechnical Institute
Sognsveien 72, NO-0806 Oslo, Norway

ABSTRACT. Besides the runout distance of an avalanche, information on avalanche intensity along the path are often required for hazard zoning or planning of mitigation measures. The avalanche (front) velocity is a common measure as it can be linked to expected impact pressures. At the same time, the velocity of an avalanche determines, if it stays in its usual track or if the avalanche unexpectedly deviates from it and thus endangers areas believed to be safe. Therefore, a reasonable prediction of the expected velocities is most important. However, many of the prevailing avalanche models tend to underestimate velocities in the track or they overestimate the runout distances. In this paper, several avalanche front velocity measurements from the Ryggfonn test site are presented. The measurements are derived from photo and/or video analyses. The measurements can be used for future model calibrations. Additionally, the measurements from the Ryggfonn test site are compared with velocity measurements from other locations to obtain a wider spectrum of avalanche conditions. By analyzing these velocities, constraints for possible rheological models of avalanche flows are obtained.

1 INTRODUCTION

Nowadays it becomes more and more common to use numerical models to predict runout distances and impact pressures for hazard mapping along potential avalanche paths. As most numerical avalanche models solve the (depth averaged) momentum or velocity equation(s), velocity measurements along the path are most important for validating those models. However, those measurements are rare, because they are difficult to obtain and often involve only point measurements. Figure 1 shows collection of velocity measurements. The line $1.8\sqrt{H}$ ($\approx 0.6\sqrt{gH}$) was proposed by McClung and Schaerer (2006) as an upper-limit envelope for the maximum velocity, mainly based on data from Rogers Pass.

Measurements along extended stretches of the avalanche tracks are only available for few sites, e.g.,

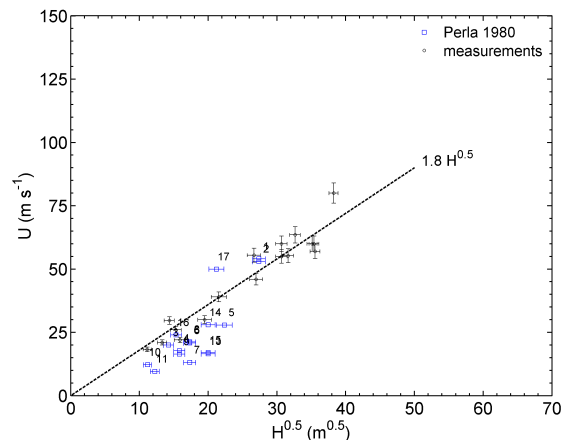


Figure 1: Avalanche velocity versus the square root of the total drop height H . Data from (Perla, 1980) along with a collection of measured maximum velocities in the middle of the track for mainly mixed-dry snow avalanches from various sites. For comparison, the line depicts the upper-limit envelope as proposed by McClung and Schaerer (2006).

*Corresponding author's address:
Peter Gauer
Norwegian Geotechnical Institute,
P.O. Box 3930 Ullevål Stadion, NO-0806 Oslo, Norway
Tel: ++47 45 27 47 43; Fax: ++47 22 23 04 48; E-mail: pg@ngi.no

(Kotlyakov et al., 1977; Gubler et al., 1986; Gauer et al., 2007b; SLF, 2006). In the following, avalanche front velocity measurements from the Ryggfonn test-site are presented. The measurements are derived from photo and/or video analyses. These measurements can be used for future model calibrations.

Additionally, the measurements from Ryggfonn are compared with (partially published) velocity measurements from other locations to obtain a wider spectrum of avalanche conditions, especially varying total drop heights.

By analyzing these velocities, constraints for rheological models for avalanche flows can be obtained.

2 OBSERVATIONS AND MEASUREMENTS

In this section some measurements from various avalanche test-sites are presented starting with data from Ryggfonn. The data involve measurements based on timed photo series and/or video analyses. For a detailed description of the different avalanche

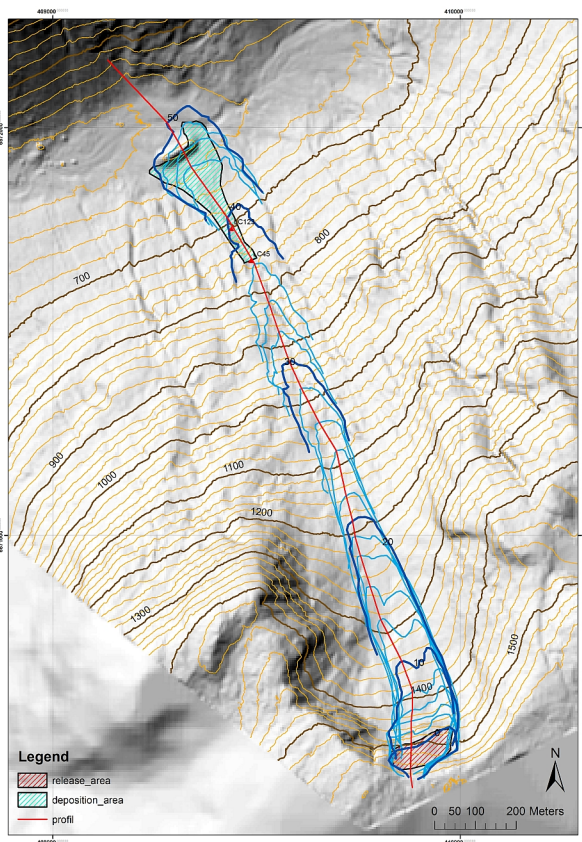


Figure 2: Ryggfonn event 1982-04-20, Stryn, Norway. Time lines of the avalanche front for every 2 s (time steps at 48 s and 52 s, are missing). The red line indicates the profile shown in Fig. 6.

test-sites the reader is referred to Barbolini and Issler (2006).

Figure 2 shows an example of the analysis of a photo series for the avalanche at the Ryggfonn test site on 20 April 1982. The corresponding velocities along the shown profile is presented in Figure 6. One should remind oneself that a representation of the front velocity along a single profile is a simplification of the three-dimensional avalanche flow. Nonetheless, it can provide a first impression of the avalanche flow.

For the purpose of comparison, the avalanche tracks are scaled by the approximated maximum drop height, H_{sc} , of the avalanche, i.e., by the maximum vertical distance that the avalanche front descend. The velocities are scaled by $\sqrt{gH_{sc}}$ to obtain a normalized velocity

$$U^* = \frac{U}{\sqrt{gH_{sc}}} \quad (1)$$

The return period of the presented avalanches ranges from about 1 year to around 50 years. Thus, they are not necessarily the design events, but some are major events relative to their path. The reference given in headings lead the reader to more detailed information of the respective event.

Ryggfonn, 2002-03-06

On 2 March 2003 a small avalanche was released at Ryggfonn test site. Figure 3 shows a snapshot after approx 17 s and Figure 4 the development of the front velocity along the main avalanche track. The velocity is derived by video analysis. The projected release area was approximately 5 250 m² and the release volume is estimated to 3 000–5 000 m³. The avalanche



Figure 3: Snapshot of the avalanche 2002-03-06 at Ryggfonn, Stryn, Norway; $t_m \approx 17$ s (video NGI).

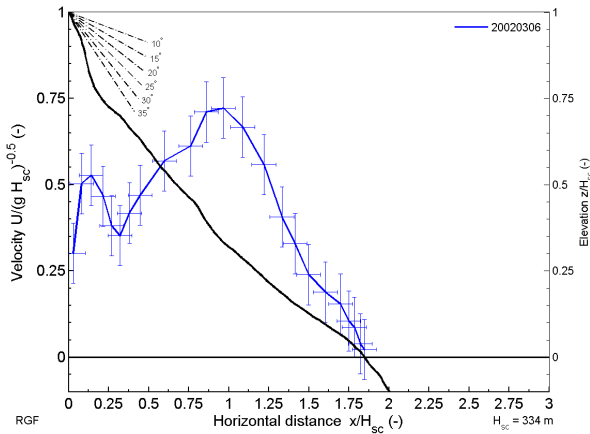


Figure 4: Velocity profile of the avalanche 2002-03-06 at Ryggfonn, Stryn, Norway. Measurements by video analysis

stopped in the cirque at a mean slope angle of about 25–30°. Its total drop height, H_{sc} , was approximately 334 m. The avalanche reached a maximum velocity of approximately 41 m s^{-1} corresponding to $0.72\sqrt{g H_{sc}}$.

Ryggfonn, 1982-04-20 (Lied, 1984)

Figure 5 shows a snapshot of the avalanche 1982-04-20 after approx 12 s. The time lines of this event are shown in Figure 2 and the corresponding velocity profile is given in Figure 4. The velocity is derived from a series of timed photographs. The powder cloud hides the underlying fluidized and dense part of the avalanche, which is narrower than the time lines in Figure 2 suggest.

At the time, the snow conditions in the path differed from dry wind packed snow in the release area to wet snow in the runout zone below approximately 800 m asl. A snow profile at the nearby Fonnbu re-

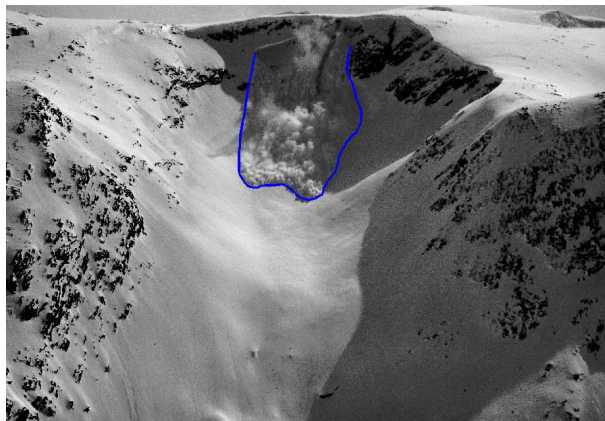


Figure 5: Snapshot of the avalanche 1982-04-20 at Ryggfonn, Stryn, Norway; $t_m \approx 12 \text{ s}$ (photo NGI).

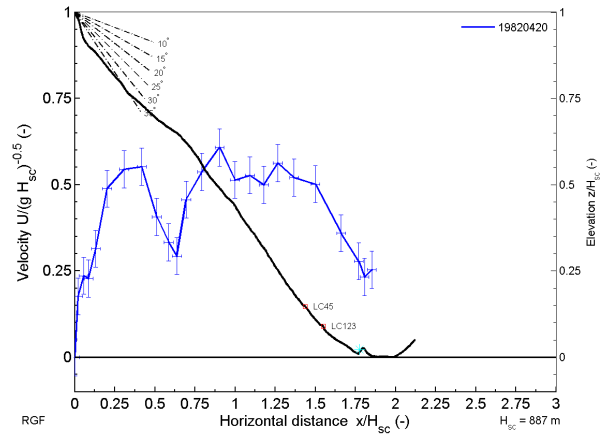


Figure 6: Velocity profile of the avalanche 1982-04-20 at Ryggfonn, Stryn, Norway. Measurements by timed photos series. The cyan * indicates the approximated end of the deposition of the fluidized or dense part.

search station (950 m asl) showed 0.7 m dry new-snow from the preceding week on top of humid old snow. The air temperatures at Fonnbu increased from -9°C to 6°C at the day of release. The projected initial release area was approximately $9\,100 \text{ m}^2$; the release volume is estimated to $11\,000\text{--}15\,000 \text{ m}^3$. A main part of the avalanche stopped just in front of the newly build catching dam. The accompanying powder cloud overtopped the dam. The total drop height was approximately 890 m. The volume of the deposits amounted to around $50\,000 \text{ m}^3$. The maximum velocity was about 57 m s^{-1} or $0.61\sqrt{g H_{sc}}$.

Ryggfonn, 2000-02-17 (Kristensen, 2001)

The avalanche on 17 February 2000 was artificially. There had been a significant increase in snow since the previous event on 11 January 2000 ($\approx 1 \text{ m}$). The top layer of the snowpack in the avalanche track consisted of about 0.3 m loose dry snow. The projected release area was about $15\,000 \text{ m}^2$ and the estimated release volume about $45\,000 \text{ m}^3$. The obvious deposition of the fluidized or dense flow amounted to approximately $80\,000 \text{ m}^3$. The avalanche destroyed the instrumentation tower LC45 and damaged the concrete wedge LC123 (cf. Gauer et al., 2007a). Figure 7 shows the avalanche shortly before it hit the instrumentation tower LC45. The measured maximum velocity was around 46 m s^{-1} corresponding to $0.5\sqrt{g H_{sc}}$. The estimated velocities are shown in Figure 8.



Figure 7: Snapshot of the avalanche 2000-02-17 at Ryggfonn, Stryn, Norway shortly before it arrives at the instrumentation tower LC45 (photo NGI).

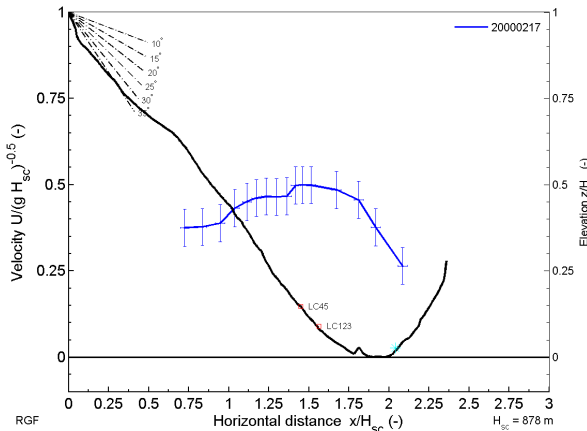


Figure 8: Velocity profile of the avalanche 2000-02-17 at Ryggfonn, Stryn, Norway. Measurements by video analysis. The cyan * indicates the approximated end of the deposition of the fluidized or dense part.

Monte Pizzac, 1994-01-08 (Nettuno, 2004)

On 8 January 1994 a first significant avalanche was released at the Italian test-site Monte Pizzac. The released volume involved approx 2000 m³ dry snow

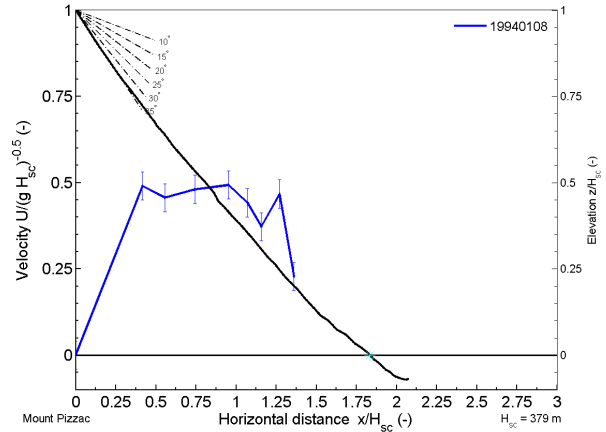


Figure 9: Velocity profile of the avalanche 1994-01-08 at Mount Pizzac, Italy. Measurements through time delays between sensor impacts (Nettuno, 2004). The cyan * indicates the approximated end of the runout zone.

with a fracture height of approx 0.5 m and a density of 210 kg m⁻³. Figure 9 shows the estimated front velocity derived from arrival time at various sensor locations. The avalanche was characterized as dry-loose snow avalanche. Its maximum velocity was probably around 30 m s⁻¹ or $0.5\sqrt{g H_{sc}}$.

Vallée de la Sionne, 1999-01-30 (SLF, 2006)

The event of 30 January 1999 was the first of three big avalanches (Fig. 10), which could be measured, at the Vallée de la Sionne during several consecutive avalanche cycles all over Europe in Winter 1999 (cf. Gruber and Margreth, 2001). After a snow-fall with 1.5 m new snow this dry-mixed avalanche was artificially released. The initial release area was approximately 52 600 m² and the fracture depth about 1.3 m amounting in a release volume of estimated 71 500 m³. The release density was measured to 200 kg m⁻³. The reported deposition volume is 39 500 m³ with an averaged density of 350 kg m⁻³ suggesting little or no entrainment (Sovilla, 2004). Figure 11 depicts a plot the normalized velocity for these events. The maximum velocity in the middle of the track was approximately 61 m s⁻¹ or $0.58\sqrt{g H_{sc}}$.

3 DISCUSSION AND CONCLUSIONS

In the preceding sections avalanche (front) velocity of avalanches with drop heights ranging from approximately 120 to 1200 m have been presented. Despite of the heterogeneous data origin, the presented front velocity show obvious similarities. In most cases the

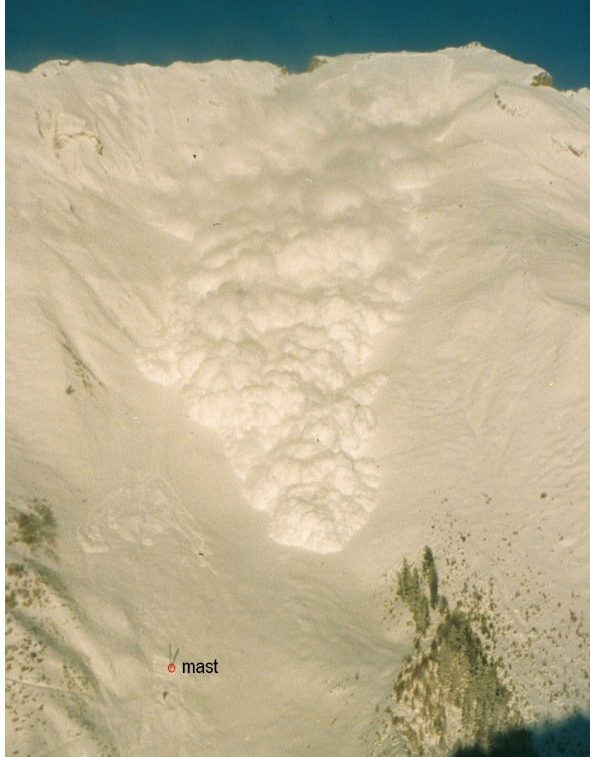


Figure 10: Avalanche 1999-01-30 (# 102) at Vallée de

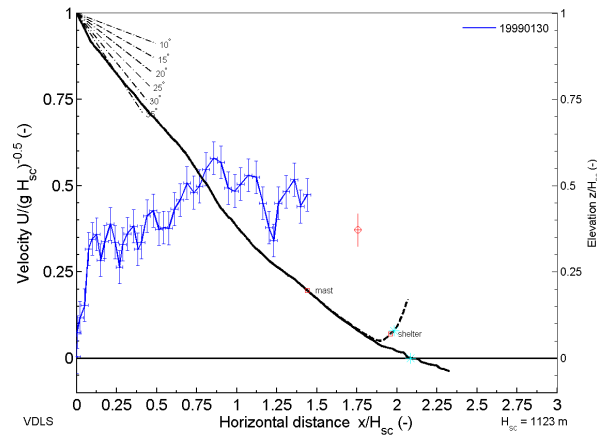


Figure 11: Velocity profile of the avalanche 1999-01-30 (# 102) at Vallée de la Sionne, Valais, Switzerland. Measurements by video analysis (SLF, 2006). The solid black line shows the avalanche track along the Sionne river and the dashed line indicates the track on the reverse slope above the shelter. The red o indicates the mean approximated mean front velocity between the mast and the shelter and the cyan * mark the approximated end of the deposition of the fluidized or dense part.

avalanche started to decelerate at slope angles between 15–30°. More importantly, the measurements

presented in the previous section as well as in Figure 1 imply that the maximum velocity of dry-mixed avalanches scale with total drop height of the path, i.e. $U_{max} \propto \sqrt{gH}$, as already suggested by McClung and Schaerer (2006). For the presented events, the maximum velocities in the middle of the track ranged between $(0.5 - 0.72)\sqrt{gH_{sc}}$.

This has implications for the choice of values for the empirical parameters in commonly used avalanche models, keeping in mind, we are interested in extraordinary events. Numerical avalanche models and the chosen empirical parameter should principally allow for this observed velocities. Assuming $U_{max} \approx 0.6\sqrt{gH}$ as proposed by McClung and Schaerer (2006), one obtains for the normalized maximum velocity in the case of a PCM-type model (Perla et al., 1980) the following relation as a first approximation:

$$U_{max}^* = \sqrt{\frac{1}{a_2 H_{sc}}} \sqrt{(\sin \phi_{U_{max}} - \mu \cos \phi_{U_{max}})}. \quad (2)$$

This means that the choice of a_2 and μ depends on the total drop height, H_{sc} , and the parameters a_2 and μ should not be chosen independently. That is maybe surprising and is contrary to common praxis, where it is often assumed that μ depends on the avalanche size and that a_2 reflects the roughness the slope and/or the effect of entrainment. Here, a_2 is the inverse of the so-called mass-to-drag ratio, M/D , μ the Coulomb friction factor, and $\phi_{U_{max}}$ is the slope angle at the point where the maximum velocity is reached. The friction factor is limited by $\mu > \tan \phi_r$, where ϕ_r is the slope angle in the runout zone of the avalanche.

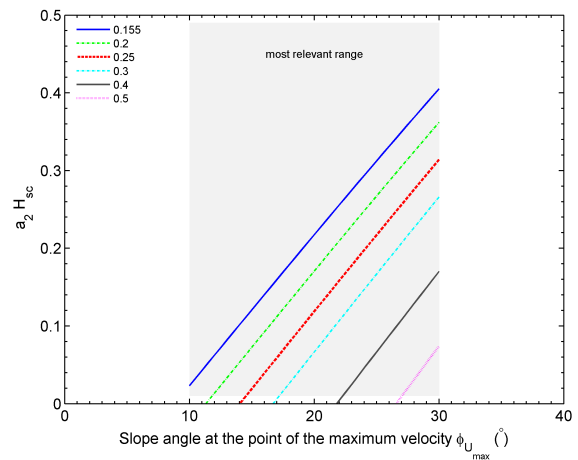


Figure 12: $a_2 H_{sc}$ versus the slope angle at the point of the maximum velocity is reached for varying values of μ and the normalized maximum velocity $U_{max}^* = 0.6$.

Figure 12 plots how $a_2 H_{sc}$ and μ are interrelated. One should recall, small a_2 values imply a more Coulomb-friction dominated flow behavior. In the case of the 2002-03-06 avalanche at Ryggfonn, which stopped at slope angle $> 25^\circ$, this might be a reasonable assumption, despite its noticeable powder cloud. However, that $U_{max} \propto \sqrt{gH}$ holds more generally suggests that the effective friction in dry-mixed avalanches is less velocity dependent as commonly believed.

Unfortunately, the relation in Equation (2) provides no unambiguous choice and needs to be supplemented by further constraints, like the expected runout distance. Though, that leads often to contradicting choices for the empirical parameter.

Similar constraints can be derived for the choice of empirical parameter values in other commonly used avalanche models (e.g. Christen et al., 2010; Sampl and Granig, 2009). However, those involve in addition the flow height, which has rarely been measured.

Velocity measurements like the presented ones combined with runout observations like (Lied and Bakkehøi, 1980; Bakkehøi et al., 1983; McClung et al., 1989; Gauer et al., 2010) constitute also constraints for the development and validation of more physically-based numerical models for dry-mixed avalanches.

ACKNOWLEDGMENTS

Parts of this research was carried out through a snow avalanche research grant to NGI from OED/NVE. Thanks to A. Zeidler for her comments on the paper.

REFERENCES

- Bakkehøi, S., U. Domaas, and K. Lied, 1983: Calculation of snow avalanche runout distance. *Annals of Glaciology*, **4**, 24–29.
- Barbolini, M. and D. Issler, 2006: Avalanche Test Sites and Research Equipment in Europe: An Updated Overview. Final-Report Deliverable D8, SATSIE Avalanche Studies and Model Validation in Europe.
- Christen, M., J. Kowalski, and P. Bartelt, 2010: RAMMS: Numerical simulation of dense snow avalanches in three-dimensional terrain. *Cold Regions Science and Technology*, **63**, 1–14, doi:DOI: 10.1016/j.coldregions.2010.04.005.
- Gauer, P., D. Issler, K. Lied, K. Kristensen, H. Iwe, E. Lied, L. Rammer, and H. Schreiber, 2007a: On full-scale avalanche measurements at the Ryggfonn test site, Norway. *Cold Regions Science and Technology*, **49**, 39–53, doi:10.1016/j.coldregions.2006.09.010.
- Gauer, P., M. Kern, K. Kristensen, K. Lied, L. Rammer, and H. Schreiber, 2007b: On pulsed Doppler radar measurements of avalanches and their implication to avalanche dynamics. *Cold Regions Science and Technology*, **50**, 55–71, doi:10.1016/j.coldregions.2007.03.009.
- Gauer, P., K. Kronholm, K. Lied, K. Kristensen, and S. Bakkehøi, 2010: Can we learn more from the data underlying the statistical $\alpha - \beta$ model with respect to the dynamical behavior of avalanches? *Cold Regions Science and Technology*, **62**, 42–54, doi:10.1016/j.coldregions.2010.02.001.
- Gruber, U. and S. Margreth, 2001: Winter 1999: A valuable test of the avalanche-hazard mapping procedure in Switzerland. *Annals of Glaciology*, **32**, 328–332.
- Gubler, H., M. Hiller, G. Klausegger, and U. Suter, 1986: Messungen an Fliesslawinen. Zwischenbericht. Internal report 41, Swiss Federal Institute for Snow and Avalanche Research.
- Kotlyakov, V. M., B. N. Rzhhevskiy, and V. A. Samoylov, 1977: The dynamics of avalanching in the Khibins. *Journal of Glaciology*, **19**, 431–439.
- Kristensen, K., 2001: The Ryggfonn Project: Avalanche data from the Winters 1996/1997, 1997/1998, 1998/1999 and 1999/2000. NGI Report 581200-33, Norwegian Geotechnical Institute, Sognsveien 72, N-0806 Oslo.
- Lied, K., 1984: Earth dams for protection against snow avalanches. Technical report, Norwegian Geotechnical Institute.
- Lied, K. and S. Bakkehøi, 1980: Empirical calculations of snow-avalanche run-out distance based on topographic parameters. *Journal of Glaciology*, **26**, 165–177.
- McClung, D. and P. Schaerer, 2006: *The Avalanche Handbook*. The Mountaineers Books, 1011 SW Klickitat Way, Seattle, Washington 98134.
- McClung, D. M., A. I. Mears, and P. Schaerer, 1989: Extreme avalanche run-out: Data from four mountain ranges. *Annals of Glaciology*, **13**, 180–184.
- Nettuno, L., 2004: Field measurements and model calibration in avalanche dynamics. *Surveys in Geophysics*, **16**, 635–648, doi:10.1007/BF00665744, ordered 20101103.
- Perla, R., T. T. Cheng, and D. M. McClung, 1980: A two-parameter model of snow-avalanche motion. *Journal of Glaciology*, **26**, 119–207.
- Perla, R. I., 1980: *Dynamics of Snow and Ice Masses*, Academic Press, New York, chapter Avalanche Release, Motion, and Impact. 397–462.
- Sampl, P. and M. Granig, 2009: Avalanche simulation with SAMOS-AT. *Proceedings of the International Snow Science Workshop, Davos*, 519–523.
- SLF, 2006: Schlussbericht Vallée de la Sionne 1998/99. Schlussbericht 260702, Swiss Federal Institute for Snow and Avalanche Research.
- Sovilla, B., 2004: *Field experiments and numerical modelling of mass entrainment and deposition processes in snow avalanches*. Diss. eth no. 15462, ETH Zurich, Zurich, Switzerland.